

## Original Paper

# Assessment of the Sensitivity to Charged Particles of Nuclear Emulsions Featuring Fine Microcrystals

Kana SAEKI<sup>a</sup>, Ken'ichi KUGE<sup>b</sup>, Tatsuhiro NAKA<sup>a\*</sup>, Takuya SHIRAIISHI<sup>c</sup>, Satoshi KODAIRA<sup>d</sup>

**Abstract:** Nuclear emulsions containing fine microcrystals typically exhibit low sensitivity to charged particles. However, the absolute assessment of the sensitivity of nuclear emulsions to charged particles based on physical quantities has not been previously addressed. A new method utilizing crystal sensitivity, defined as the ratio of the number of developed silver grains to the number of silver halide microcrystals per unit length traversed by charged particles, is proposed. Two types of emulsion plates with crystal sizes of 70 nm and 200 nm were irradiated with four different types of charged particles with various energy deposition. The crystal sensitivity increased with increasing energy deposition in both emulsions. Notably, the crystal sensitivity of the 70 nm size was lower than that of the 200 nm size. The crystal sensitivity of the former saturated at approximately 50%, even though the latter at 100%. This low sensitivity can be attributed to significant recombination of electron-hole pairs and, to some extent, re-halogenation enhanced in small crystals.

**Key words:** Nuclear emulsion with silver halide microcrystals, Ultrafine microcrystals, Crystal sensitivity, High-energy charged particle, Recombination

## 1. Introduction

Nuclear emulsions, utilized as solid-state track-detectors for charged particles, belong to the category of silver halide photosensitive materials. They consist of a film or plate coated with a gelatin layer in which silver halide microcrystals, serving as sensors, are dispersed. As charged particles traverse these crystals, silver ions are reduced by the energy and latent image specks are created similar to those produced by light exposure. During the development process, these silver halide microcrystals with latent image specks are converted preferentially into silver grains. These developed silver grains, aligned with the path of a charged particle, form a visualized track.

Nuclear emulsions offer exceptionally high spatial resolution, down to the sub-micrometer level, for track analysis. This remarkable resolution is attributed to the size of the silver halide microcrystals, which are typically sub-micrometer in size. As the resolution of nuclear emulsions is directly linked to the size of these microcrystals. A fine-grained nuclear emulsion of NIT (Nano Imaging Tracker) was employed. Developed originally for the search of dark matter, the NIT emulsion features ultrafine silver halide microcrystals of 70 nm in size<sup>1)</sup>. Compared to conventionally used nuclear emulsions, such as those utilized in the OPERA experiment with crystal sizes around 200 nm<sup>2)</sup>, the NIT emulsion offers higher spatial resolution.

The NIT emulsion has previously been integrated into experiment focused on directional dark matter search<sup>3)</sup>.

The sensitivity of nuclear emulsion is typically adjusted to ensure detection capability for MIPs (Minimum Ionizing Particles). To achieve this, emulsions are commonly treated with gold and sulfur sensitization. However, the NIT emulsion is not sensitive to MIPs and is primarily designed for detecting highly ionized particles. It targets particles with an energy deposition at least 20 times greater than that of MIPs, and these particles typically possess more energy than the one that a single MIP generates. The detection performance for MIPs correlates closely with photosensitivity, and photographic sensitometry was utilized during the development of the OPERA film.<sup>4)</sup> On the other hand, it has been reported that the sensitivity is proportional to the volume of microcrystals under suitable light exposure conditions.<sup>5) 6)</sup> This relationship exists because the number of photons absorbed and the number of electron-hole pairs generated are both proportional to the volume of a crystal.

Ihama reported a case of radiation exposure where the latent image formation process induced by high-energy electromagnetic-waves, such as X-rays, exhibited similarities to that of high-intensity light-exposure<sup>7) 8)</sup>, although the emulsion used did not consist of ultrafine microcrystals. On a related note, high-intensity reciprocity-law failure often occurs in such high intensity exposures, leading

Received 8th May, 2024; Accepted 27th September, 2024; Published 12th November, 2024

<sup>a</sup> Toho University

2-2-1 Miyama, Funabashi-City, Chiba, 274-8510, Japan

<sup>b</sup> Chiba University

1-33 Yayoi-cho, Inage-ku, Chiba-City, Chiba, 263-8522, Japan

<sup>c</sup> Kanagawa University

3-27-1 Rokkakubashi, Kanagawa-ku, Yokohama-City, Kanagawa, 221-8686, Japan

<sup>d</sup> National Institutes for Quantum Science and Technology

4-9-1, Anagawa, Inage-ku, Chiba-City, Chiba 263-8555, Japan

\* Corresponding author

to a decrease in sensitivity. This failure can be attributed to the simultaneous production of a large number of electron-hole pairs, which increases the recombination of electron-hole pairs and also enhances a higher dispersion of latent image specks. This dispersion leads to the formation of many undevelopable latent sub-image specks.

Therefore, quantitative understanding of the sensitivity to charged particles in NIT is crucial for comprehensively grasping its detection performance. There is a concern that nuclear emulsions containing fine microcrystals may exhibit lower sensitivity to radiation compared to conventional nuclear emulsions with larger crystals, similar to the behavior observed with light. As charged particles traverse the microcrystals, numerous electron-hole pairs are generated within approximately 1 femtosecond. Research on the relationships between such dense electronic-excitation and the efficiency of latent image formation is anticipated. The objective of this study is to investigate the efficiency of latent image formation at NIT under conditions of high-density of electronic-excitation. This will be achieved by quantitatively evaluating sensitivity using charged particles with known energy deposition. In this study, high-energy ion beam of several hundred MeV/u were employed for this purpose.

Grain Density (GD), defined as the number of silver grains formed by the development per unit length of a track, is commonly used to evaluate sensitivity to charged particles. However, GD is not an absolute evaluation based on physical quantities because it is influenced by the preparation conditions of the emulsion, such as the density of emulsion layer or the crystal size. Comparing the sensitivity to charged particles among nuclear emulsions with varying properties can be challenging.

We propose a new method called “crystal sensitivity” in this paper as a means to evaluate the sensitivity to charged particles. Crystal sensitivity is defined as the ratio of the number of developed silver grains to that of silver halide microcrystals traversed by a charged particle per unit length. This evaluation method is independent of the density and crystal size of nuclear emulsions, enabling the abso-

lute evaluation of emulsion sensitivity to charged particles with high energy deposition.

Here, we present our analysis of the difference in crystal sensitivity arising from variations in crystal size (specifically, 70 nm and 200 nm) and the amount of energy deposition of charged particles.

## 2. Experimental Methods

Two types of nuclear emulsions were used to evaluate the crystal sensitivity. One was a fine-grained nuclear emulsion (NIT) composed of silver iodobromide microcrystals with a spherical shape and a diameter of  $\sim 70$  nm. The density of the dried emulsion layer was about  $3.1 \text{ g/cm}^3$ . The other emulsion, LGE (Larger Grain Emulsion), shared the same halogen composition as NIT but had a crystal size of around 200 nm. However, the density was similar to  $3.1 \text{ g/cm}^3$ . This emulsion was an improved version of the OPERA-type emulsion. The diameter of the microcrystals was measured using electron-micrographs captured with a transmission electron microscope and analyzed with image processing software Image J. The distribution of the diameter is depicted in Fig. 1. The average diameter of the crystals in NIT was found to be  $67 \pm 9$  nm, whereas that of LGE was  $212 \pm 12$  nm.

The emulsion plates used were prepared as follows: 2 ml of melted emulsion was poured onto a slide glass ( $26 \times 76$  mm), covering the entire area, and then dried in a dark room at the conditioning temperature (ca.  $20^\circ\text{C}$ ). The thickness of the dried emulsion plate was about  $30 \mu\text{m}$  under these pouring conditions. Halogen-acceptor sensitization was conducted by immersing the dried plates in a solution of sodium sulfite ( $5 \text{ g/L}$ ) at  $20^\circ\text{C}$  for 15 minutes.

These vacuum-packed plates were irradiated with a high-energy ion beam parallel to the plate surface using the Heavy Ion Medical Accelerator in Chiba (HIMAC) at the National Institute for Quantum Science and Technology (QST). We used four beams consisting of different nuclides and energy depositions ( $dE/dx$ ). Table 1 shows the nuclides in the ion beam, their respective kinetic energies, energy

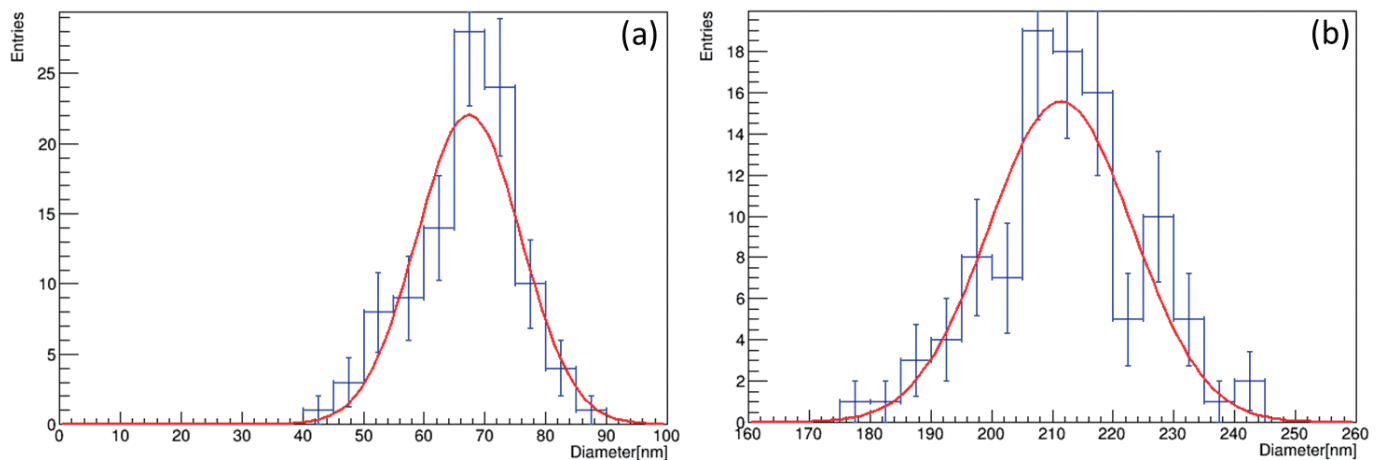


Fig. 1. Distribution of the crystal size for each emulsion obtained from transmission-electron micrographs analyzed with image processing software of Image J. (a) NIT, (b) LGE.

Center value of fitting parameter of NIT microcrystals = 67 nm, standard deviation = 9 nm, for statistic number = 102, and of LGE microcrystals = 211 nm, standard deviation = 12 nm, for statistic number = 100.

Approximation curves with red line are obtained by Gaussian fitting.

losses in silver bromide, and the number of electron-hole pairs generated when the nuclide passes through the center of a silver bromide microcrystal with a diameter of 70 nm. The number of electron-hole pairs was calculated by dividing the energy loss in a crystal by the energy of 5.8 eV<sup>9)</sup>, which is required for the formation of one electron-hole pair.

We developed the irradiated plates by immersing in a solution of Metol Ascorbic Acid developer<sup>10)</sup> at a temperature of  $5.0 \pm 0.2$  °C for 10 minutes. The number of developed silver particles per unit length of the track was counted visually using a reflected light-microscope.

### 3. Evaluation method

The number of silver halide microcrystals per unit length of the path traversed by a charged particle in the emulsion layer was calculated under the assumption of random distribution of microcrystals. Typically, the microcrystals in the layer are densely dispersed, and their number density depends on factors such as crystal size and emulsion density, which represents the weight ratio of microcrystals in the layer. The average spacing between the crystals in the layer was estimated to be about 50 nm. However, after development, the size of silver grains formed is larger than that of the original silver halide microcrystals, resulting in a shortened average spacing of about 20 nm. This spacing is too short to count accurately the number of developed silver grains on the track using a standard optical system with a resolution of about 240 nm. To facilitate grain counting by spreading out the grains, we prepared six diluted emulsions with varying densities of crystal numbers by adding a gelatin solution (2.6 mass%), which served as the same binder as the original emulsion. Additionally, this treatment aimed to confirm that the crystal sensitivity remained independent of the dilution ratio, thereby ensuring

Table 1. Nuclides of irradiated ions, energy, energy of ion, energy loss in silver bromide and number of electron-hole pairs generated when the nuclides traverses through the center of a silver-bromide microcrystal of 70 nm diameter.

Nuclide	Energy [GeV]	dE/dx [keV / 10 nm]	Number of electron-hole pairs produced
He	0.6	0.14	110
C	3.48	0.51	620
Ar	20	3.78	4560
Fe	28	7.47	9010

Table 2. Amount of gelatin solution (2.6 mass%) added to 1 ml of NIT emulsion, the density of NIT emulsion after drying, and the number of crystals traversed by a charged particle per 1  $\mu\text{m}$ .

Amount of gelatin solution added to 1 ml of NIT [ml]	Density of NIT after drying [g/cm <sup>3</sup> ]	N [ $\mu\text{m}$ ]
0	$3.08 \pm 0.01$	$8.6 \pm 0.3$
2.1	$2.03 \pm 0.01$	$3.5 \pm 0.2$
4.7	$1.73 \pm 0.01$	$2.1 \pm 0.1$
6.6	$1.65 \pm 0.01$	$1.7 \pm 0.1$
10.7	$1.54 \pm 0.01$	$1.1 \pm 0.1$
23.3	$1.43 \pm 0.01$	$0.6 \pm 0.1$

the validity of the evaluation method using crystal sensitivity. The amounts of the gelatin solution added are detailed in Table 2.

To calculate the number of silver halide crystals traversed by the charged particle, it is necessary to determine the emulsion density for each dilution. This was measured as follows: The emulsion layer consists of both gelatin and silver halide, and only gelatin remains after fixation. The weight difference of the dried emulsion before and after fixation indicates the weight of silver halide, allowing us to obtain the weight ratio of gelatin to silver halide, which determines the emulsion density. We disregarded the trace of water remaining in the emulsion layer after drying, as the amount of water remaining after sufficient drying was negligible. Measurements of water traces in both air-dried and forced-dried cases showed agreement within the margin of error. It can be assumed that there is no significant difference in the density of emulsions dried in air compared to those set in the vacuum-packing during irradiation of charged particles.

From these results, we obtained the volume ratio of silver halide in the layer. We then calculated the number of crystals in the volume of a cylinder with the same radius as the microcrystal and a height of 1  $\mu\text{m}$  using this ratio. This value represents the number of microcrystals per unit length in the emulsion layer, and we defined it as the number of crystals traversed by a charged particle per unit length.

The number of developed silver grains per unit length was counted. Subsequently, we plotted the relationship between the number of silver grains and the number of silver halide microcrystals per unit

Table 3. Amount of GD and crystal sensitivity for plates coated with NIT emulsion at different rates of gelatin solution for an irradiation of each charged particle.

Helium		
Density of NIT after drying[g/cm <sup>3</sup> ]	GD [ $\mu\text{m}$ ]	Crystal Sensitivity [%]
$3.11 \pm 0.01$	$0.53 \pm 0.02$	$8.2 \pm 0.5$
$2.01 \pm 0.01$	$0.23 \pm 0.02$	$9.0 \pm 0.6$
Carbon		
Density of NIT after drying[g/cm <sup>3</sup> ]	GD [ $\mu\text{m}$ ]	Crystal Sensitivity [%]
$3.08 \pm 0.01$	$1.23 \pm 0.02$	$14.7 \pm 0.6$
$2.03 \pm 0.01$	$0.56 \pm 0.01$	$16.1 \pm 0.8$
$1.73 \pm 0.01$	$0.38 \pm 0.01$	$18.5 \pm 1.1$
$1.65 \pm 0.01$	$0.23 \pm 0.01$	$13.8 \pm 1.0$
$1.54 \pm 0.01$	$0.11 \pm 0.01$	$9.3 \pm 1.0$
$1.43 \pm 0.01$	$0.07 \pm 0.02$	$12.0 \pm 3.2$
Argon		
Density of NIT after drying[g/cm <sup>3</sup> ]	GD [ $\mu\text{m}$ ]	Crystal Sensitivity [%]
$1.65 \pm 0.01$	$0.72 \pm 0.02$	$43.2 \pm 3.0$
$1.54 \pm 0.01$	$0.47 \pm 0.01$	$41.3 \pm 3.0$
$1.43 \pm 0.01$	$0.17 \pm 0.01$	$27.9 \pm 2.6$
Iron		
Density of NIT after drying[g/cm <sup>3</sup> ]	GD [ $\mu\text{m}$ ]	Crystal Sensitivity [%]
$1.73 \pm 0.01$	$1.08 \pm 0.02$	$51.9 \pm 2.9$
$1.65 \pm 0.01$	$0.87 \pm 0.01$	$52.2 \pm 3.5$
$1.54 \pm 0.01$	$0.50 \pm 0.01$	$43.6 \pm 3.1$
$1.43 \pm 0.01$	$0.23 \pm 0.01$	$36.9 \pm 3.5$

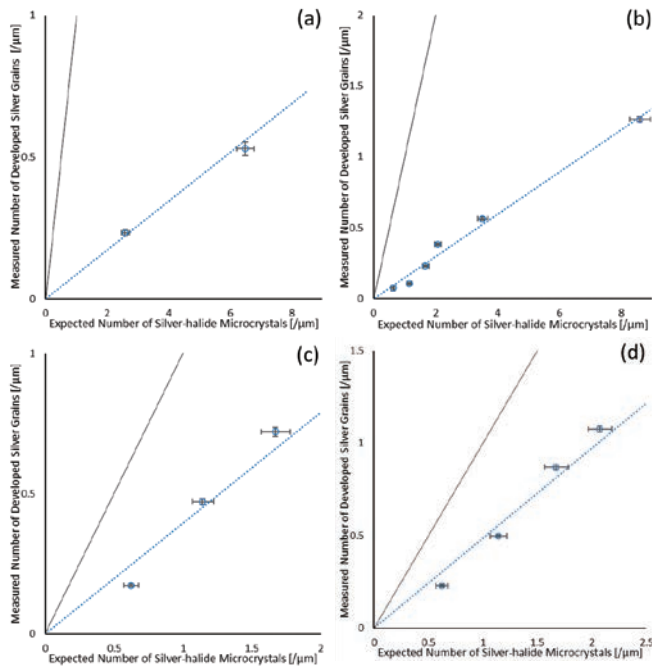


Fig. 2. Relationships between the number of developed silver grains and that of silver halide microcrystals traversed by each charged particle per unit length in the NIT emulsion layer. Dotted lines are the ones passing through the plotting points. The slopes of these lines represent the crystal sensitivity. Solid lines are the ones with a slope of unity, corresponding to the crystal sensitivity of 100% (a) helium (0.6 GeV), (b) carbon (3.48 GeV), (c) argon (20 GeV), (d) iron (28 GeV)

length. A straight line was drawn through these plotted points, and the slope of this line represents the crystal sensitivity. The error associated with the crystal sensitivity was estimated using the chi-square method with a 90% confidence interval.

4. Results

The relationships between the number of developed silver grains and that of silver halide microcrystals per unit length of a track in the NIT emulsion layers at different dilution rates are summarized in Table 3 and depicted in Fig. 2 for each charged particle listed in Table 1. Straight and dotted lines passing through the plotted points are shown. Crystal sensitivities were obtained from the slopes of these lines determined using the chi-square goodness-of-fit test. The solid line represents a straight line with a slope of 1, corresponding

Table 4. Amount of GD and crystal sensitivity for plates coated with LGE emulsion at different dilution rates of gelatin solution for an irradiation of each charged particle.

Helium		
Density of LGE after drying[g/cm <sup>3</sup> ]	GD [μm]	Crystal Sensitivity [%]
2.67 ± 0.01	1.04 ± 0.06	55.7 ± 3.6
Carbon		
Density of LGE after drying[g/cm <sup>3</sup> ]	GD [μm]	Crystal Sensitivity [%]
1.67 ± 0.01	0.35 ± 0.03	77.7 ± 6.6
1.52 ± 0.01	0.24 ± 0.02	88.6 ± 7.2

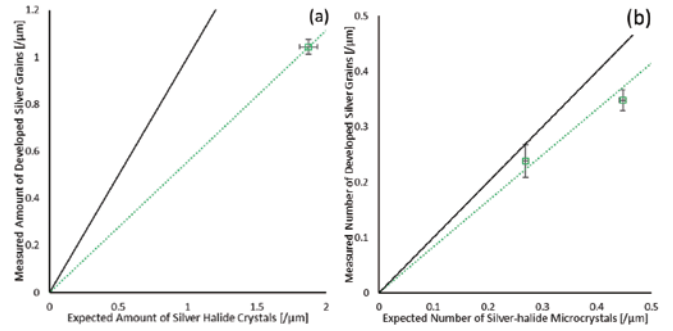


Fig. 3. Relationships between the number of developed silver grains and that of silver halide microcrystals traversed by each charged particle per unit length in the LGE emulsion layer. Dotted lines are the ones passing through the plotting points. The slopes of these lines represent the crystal sensitivity. Solid lines are the ones with a slope of unity, corresponding to the crystal sensitivity of 100% (a) helium, (b) carbon

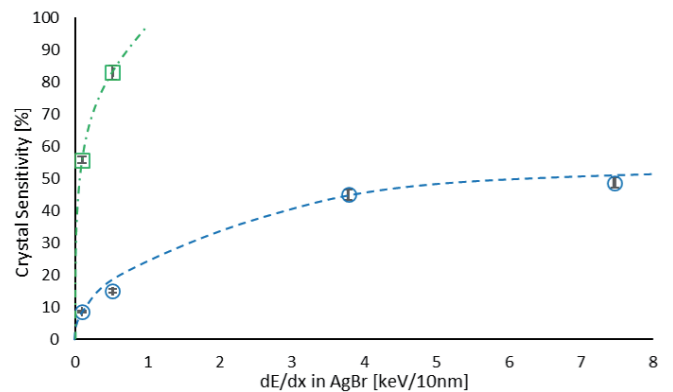


Fig. 4. Relationships of the crystal sensitivity to the amount of energy loss in silver bromide irradiated with different charged particles. Circles and dashed line = NIT, Squares and chain line = LGE. Both lines were drawn freehand to pass through the plotted points.

to a crystal sensitivity of 100%.

The error in the number of silver halide microcrystals arises from measurement errors in the emulsion density after drying and in the diameter of the microcrystals. The error in the number of developed silver grains comes from the statistical error associated with the measured number of grains. As the dotted lines in Fig. 2 demonstrate good linearity, it can be inferred that the crystal sensitivity in NIT is independent of the dilution ratio. This finding ensures the validity of the proposed method. Consequently, we reduced the sample number of diluted LGE emulsions based on this result.

Similar relationships for both helium and carbon ions in the emulsion layers of LGE are summarized in Table 4 and depicted in Fig. 3. The slopes observed for LGE emulsions are larger than those for the NIT emulsions.

The relationships between the crystal sensitivity obtained from the results in Figs. 2 and 3 and the amount of energy loss for each ion in silver halide, as listed in Table 1, are depicted in Fig. 4. Both lines were drawn freehand to pass through the plotted points. It is observed that the crystal sensitivity increases with the amount of energy loss, and the LGE emulsion demonstrates higher sensitivity compared to the NIT one. Notably, the crystal sensitivity for the NIT emulsion saturates at around 50% even with an increase in en-

ergy loss. This suggests that only about half of the crystals are developed, despite the fact that the number of electron-hole pairs produced from one ion passing through a crystal can reach a maximum of 9000 for Fe ions, as shown in Table 1. This number should be sufficient to produce developable latent image specks, considering that the minimum number of silver atoms required to produce a developable latent image speck was estimated to be four<sup>11)</sup>.

## 5. Discussion

The difference in crystal sensitivity between NIT and LGE for high-energy charged-particle irradiations is examined as follows, considering the similarity between radiation irradiation and high-intensity light exposure<sup>7)</sup>, as well as the phenomenon of high-intensity reciprocity-law failure.

Takada explored the causes of this high-intensity reciprocity-law failure, highlighting factors such as ionic limitation, competitive nucleation, topographic effects, and recombination effects.<sup>12)</sup>

The concept of ionic limitation suggests that the efficiency of latent image formation decreases with decreasing the ionic conductivity. This occurs because the period required for interstitial silver ions to reach the electrons captured in the electron trap is prolonged, leading to an increase in loss of electrons during this period. However, the larger specific surface area of crystals in NIT compared to those in LGE would result in the increase in conductivity due to a high production of interstitial silver ions from the surface. Therefore, this explanation may not fully account for the observed differences in crystal sensitivity between NIT and LGE.

Competitive nucleation induces the dispersion of latent image specks, resulting in the formation of numerous small undevelopable silver specks, to decrease in sensitivity. However, the crystals in NIT may not be large enough to cause significant dispersion of latent image specks. It remains unclear whether dispersion occurs and contributes to the sensitivity differences observed.

The topographic effect involves a competition of electron capturing between the surface and the interior of the crystal. This effect is intensified during high-intensity exposure because shallow traps in the interior of the crystal would be used as sites for the formation of silver atoms, leading to a decrease in surface sensitivity. However, since the internal latent images are rarely formed in NIT emulsions due to the small crystal size, the decrease in surface sensitivity is unlikely to occur.

Regarding the recombination effect, Takada suggested that the latent image formation proceeds through a first-order reaction rate to intensity, while recombination proceeds through a second-order reaction rate. Therefore, latent image formation is considered to occur in a primary reaction to exposure value, while recombination occurs as a secondary reaction.<sup>12)</sup> In general, the former depends solely on an electron concentration, while the latter depends on the product of electron and hole concentrations. Both concentrations are nearly equal immediately after their generations. In the case of light exposure, the concentrations of electrons or holes do not depend on the crystal size since the numbers of both are proportional to the volume of the crystal<sup>5)</sup>. However, in the case of charged par-

ticles, both numbers depend on the passage range of the particle through the crystal, thus being proportional to the crystal diameter. As the concentrations of both are the quotient of the number of electrons or holes divided by the volume of crystal, they are inversely proportional to the square of the crystal diameter. Therefore, the product of electron and hole concentrations for one hit of charged particles becomes larger in NIT with a smaller crystal size than in LGE. Consequently, the recombination probability would be higher in NIT, leading to the decrease in sensitivity.

The space charge layer serves to separate the charge by drifting holes to the crystal surface and electrons to the bulk, thereby reducing recombination. However, the thickness of the space charge layer in silver bromide is estimated to be 60 nm<sup>13)</sup>. Therefore, the crystals in NIT with a diameter of 70 nm may not have a sufficient bulk area, leading to inadequate charge-separation and increase in recombination. Conversely, the crystals in LGE with a diameter of 200 nm possess an effective space charge layer, aiding in the decrease in recombination.

Considering the difference in sensitivity between NIT and LGE from the perspective of high-intensity reciprocity-law failure, the lower crystal sensitivity in NIT can largely be attributed to the recombination effects caused by the high concentrations of both electrons and holes.

In addition, we also considered the contribution of re-halogenation, a factor not mentioned by Takada<sup>12)</sup>. Re-halogenation occurs as halogen atoms produced from holes arrive at the crystal surface. When considering the halogen concentration per unit surface area of crystals with different sizes, this concentration is inversely proportional to the diameter of the crystal, as discussed above. Therefore, the halogen concentration per unit surface area is higher for NIT with smaller crystal sizes compared to LGE. This indicates that NIT is more susceptible to re-halogenation than LGE. However, halogen-acceptor sensitization (HA sensitization) has been found to be effective in preventing re-halogenation in ultrafine-grain emulsions, as previously reported<sup>6)</sup>. The HA sensitization, which would effectively suppress re-halogenation, was also used in this experiment. Therefore, the contribution to the decrease in sensitivity due to re-halogenation is expected to be minimal. For further details on the mechanism and effects, refer to reference 14.

The difference in sensitivity between NIT and LGE could mainly be attributed to recombination due to the difference in concentrations of electron and hole, and partly due to the absence of a space charge layer and the re-halogenation. Recombination would significantly impact the decrease in sensitivity for NIT, as evidenced by its saturation in crystal sensitivity at around 50%, whereas LGE exhibited significantly higher crystal sensitivity.

For dark matter search using NIT, the detection target is low-velocity nuclei recoiled by dark matter. These recoil nuclei are expected to have velocities of approximately  $10^{-3}$  times the speed of light and lose their charge, becoming neutralized in the medium. Then they move as neutral atoms. However, such low-velocity atoms indicate high latent-image-formation efficiency<sup>15)</sup>, and we expect some unique mechanisms similar to those observed in high-energy ions such, as discussed in this report. This forms the basis of our next re-

search focus.

## 6. Conclusion

A new method for evaluating the sensitivity of nuclear emulsions to high-energy charged-particles has been proposed. This method enables direct comparison of sensitivity between emulsions with different crystal sizes and other characteristics. In this study, we directly evaluated the crystal sensitivities of NIT (crystal size of 70 nm) and LGE (crystal size of 200 nm), where NIT exhibited remarkably low crystal sensitivity. The crystal sensitivity increased along with the energy loss of high-energy ions for both emulsions. However, in the case of NIT, the sensitivity saturated at approximately 50%, despite the expected generation of a sufficient number of electron-hole pairs

to render crystals developable. We have explored several potential reasons for this low sensitivity and concluded that recombination was the primary cause. Recombination in NIT with smaller crystal size proceeds significantly due to the large concentrations of electrons and holes.

## Acknowledgements

This work was conducted as part of the accelerator experiments of Research Project H212 at QST-HIMAC. We extend our gratitude to the accelerator operators for their generous support throughout the experiments. This work was supported by the Japan Society for the Promotion of Science (JSPS) KAKENHI Grants No. JP18H03699, No. JP19H05806, No. JP24H02241.

## References

- 1) T. Asada, T. Naka, K. Kuwabara, M. Yoshimoto, *Prog. Theor. Exp. Phys.*, **2017**, 063H01 (2017).
- 2) T. Nakamura, A. Ariga, T. Ban, T. Fukuda, and 31 others, *Nucl. Instrum. Methods Phys. Res.*, **556**, 80 (2006).
- 3) T. Naka, *J. Soc. Photogr. Sci. Tech. Jpn.*, **78**, 218 (2015), (in Japanese).
- 4) K. Kuwabara, S. Nishiyama, *J. Soc. Photogr. Sci. Tech. Jpn.*, **67**, 521 (2004), (in Japanese).
- 5) T. Tani, *J. Imaging Sci.*, **29**, 93 (1985).
- 6) K. Kuge, T. Tsutsumi, K. Morimoto, Soc Man Ho Kimura, T. Suzuki, T. Mitsuhashi, A. Hasegawa, *J. Imaging Sci. Tech.*, **53**, 010507 (2009).
- 7) M. Ihama, *J. Soc. Photogr. Sci. Tech. Jpn.*, **67**, 532 (2004), (in Japanese).
- 8) M. Ihama, *J. Soc. Photogr. Sci. Tech. Jpn.*, **76**, 333 (2013), (in Japanese).
- 9) K. A. Yamakawa, *Phys. Rev.*, **82**, 522 (1951).
- 10) A. Umemoto, T. Naka, T. Nakano, R. Kobayashi, T. Shiraishi, T. Asada, *Prog. Theor. Exp. Phys.*, **2020**, 103H02 (2020).
- 11) P. Fayet, F. Granzer, G. Hegenbart, E. Moisar, B. Pischel, L. Woste, *Phys. Rev.*, **55**, 27 (1985).
- 12) S. Takada, *J. Soc. Photogr. Sci. Tech. Jpn.*, **42**, 112 (1979), (in Japanese).
- 13) S. Yamashita, N. Ohshima, S. Takada, K. Kuge, *J. Soc. Photogr. Sci. Tech. Jpn.*, **78**, 174 (2015), (in Japanese).
- 14) T. Tani, T. Uchida, T. Naka, *Rad. Meas.* **129**, 106184 (2019).
- 15) M. Natsume, K. Hoshino, K. Kuwabara, M. Nakamura, T. Nakano, K. Niwa, O. Sato, T. Tani, T. Toshito, *Nucl. Instrum. Methods Phys. Res.*, **575**, 3 (2007).